Conference Proceedings

EuroSun 2014
Aix-les-Bains (France), 16 – 19 September 2014

SEASONAL THERMAL ENERGY STORAGE WITH AQUEOUS SODIUM HYDROXIDE - REACTION ZONE DEVELOPMENT, MANUFACTURING AND FIRST EXPERIMENTAL ASSESSMENTS.

Xavier Daguenet-Frick[1], Paul Gantenbein[1], Elimar Frank[1], Benjamin Fumey[2], Robert Weber[2], Tommy Williamson[3].

[1] SPF-HSR, Eichwiesstrasse 20, 8645 Rapperswil-Jona, Switzerland.

[2] EMPA, Überlandstrasse 129, 8600 Dübendorf, Switzerland.

[3] Kingspan Environmental Ltd, 180 Gilford Road, Portadown, Craigavon BT63 5LF, United Kingdom./company, city

Abstract

In this paper, the theoretical and experimental investigation of the reaction zone construction of an absorption/desorption concept with sodium hydroxide (NaOH) and water is described. Both heat and mass exchangers – absorber/desorber (A/D) and evaporator/condenser (E/C) - constituting this reaction zone are falling film tube bundles working under reduced pressure (evacuated container). The different choices made for the construction of the reaction zone are outlined: the container as well as the manifold design, the vapour pathway with thermal radiation protection, the liquid level measurement cell and the tube bundle are described. After construction of the reaction zone, the work was focused on the first assessment of the A/D and E/C units in order to check their proper functioning. In this context, Helium leakage tests were carried out for the different components and an optical setup enabling to check the efficiency of the manifold with a substituted fluid is realized for the A/D unit.

Keywords: tube bundle, falling film, absorption, desorption, sodium lye, vacuum, seasonal thermal energy storage, solar thermal energy.

1. Introduction

Seasonal storage using sensible thermal energy in materials (usually water) has two main disadvantages: comparably high thermal losses and a low volumetric energy density (Duffie and Beckman 2013). A process involving absorption and desorption could be a solution to improve both aspects.

In the absorption/desorption storage concept with sodium hydroxide (NaOH) and water, the energy provided by the solar collectors (solar heat, see Fig. 1) during charging process in summer is used to vaporize under reduced pressure a portion of the water contained in the diluted caustic soda solution (desorber). Then, the latent condensation heat (condenser) is released to the ground by means of a bore hole (heat sink) and the liquid water as well as the concentrated solution generated are separately stored at room temperature. During discharging, the process is reversed: The ground heat (heat source) is used to evaporate the water under reduced pressure (evaporator) and the absorption of the vapour into the concentrated caustic soda solution releases heat (absorber) at a temperature level sufficiently high to satisfy the building's heating and domestic hot water production requirements in winter time (Weber and Dorer 2008).

Selection and/or peer review under responsibility of EuroSun2014 Scientific Committee
doi:10.18086/eurosun.2014.10.08 Available at http://proceedings.ises.org

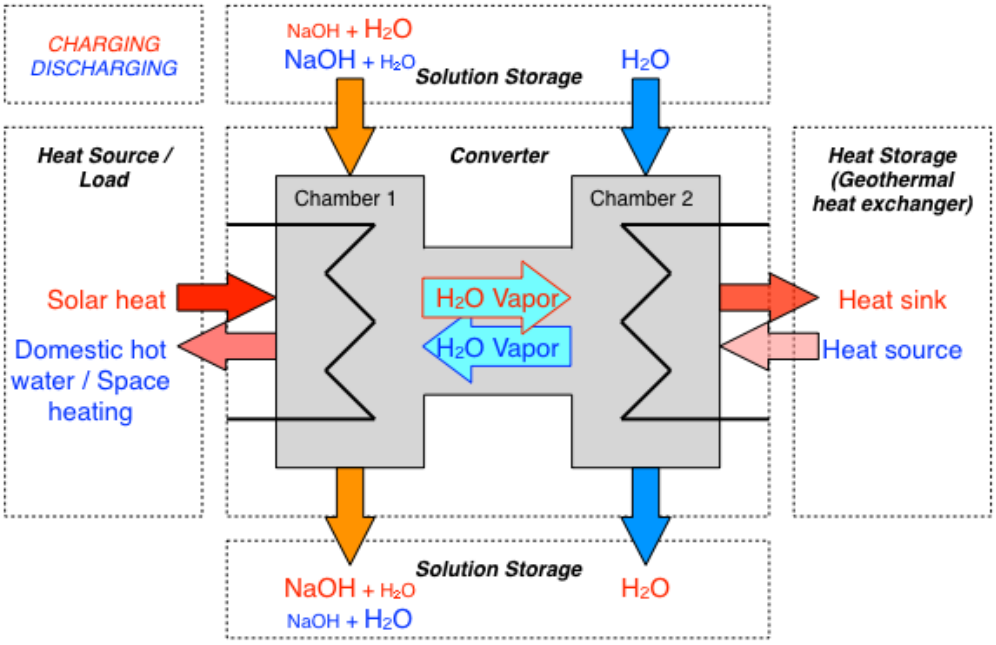

Fig. 1: The concept of the closed sorption heat pump based heat storage (Fumey et al. 2014).

To perform this storage concept, heat and mass exchangers are core components in the system design; after having described the layout and the component improvement of the Absorber/Desorber reaction zone (Daguenet-Frick et al. 2013), the present study will focus on the manufacturing and on the first assessments of the reaction zone.

2. Reaction zone construction

The seasonal sequential operation of the heat storage allows the combination of the process stages – absorption and desorption – (absorber and desorber unit) and evaporation and condensation (evaporator and condenser unit) each in one component (A/D unit presented on the left part of Fig. 2, E/C unit on the right), leading to a decrease of the volume and hence to an increase of the volumetric energy density of the storage system.

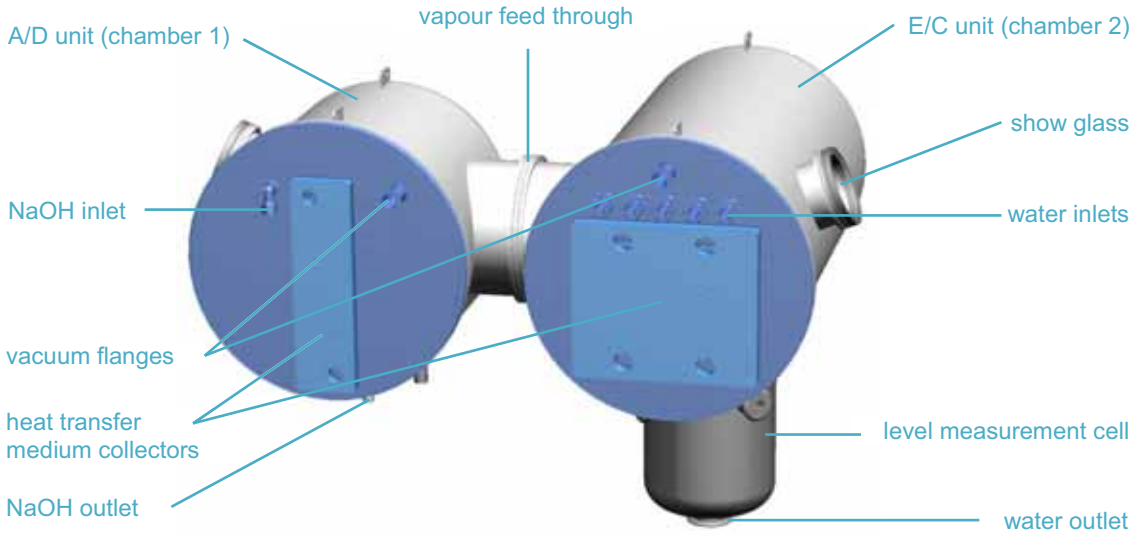

Fig. 2: CAD drawing of the reaction zone with both A/D (left) and E/C unit (right).

Due to the high heat and mass exchange abilities of tube bundle heat and mass exchangers, a technology presenting a good compactness is used for both heat and mass exchangers.

Both tube bundles - of the A/D and the E/C - are designed in order to fit, assembled with their manifold in a

400 mm stainless steel tube container ensuring the reaction zone working under reduced pressure. The processes are running in the absence of air and therefore a not leaking vacuum envelope is required. To prevent gases -air- leaking into the vacuum chambers, as much as possible of the vessels are welded out of standard parts available on the market supplied by appropriate manufacturers. To keep experimental flexibility most of the feed through have a gasket tightening.

A modular concept (each component is easily dismountable) as well as a limited number of vacuum sealing gaskets were two challenges in the container design. As showed on Fig. 2, two inspection glasses allow the view at the top of the tube bundles, directly under the feed manifold. Except the both fluid outlets at the bottom of the containers and a temperature sensor feed through in the A/C envelope, all connections and feed thoughts are located on the tube bundles flanges (in blue on Fig. 2). These connections enable the feed of the tube manifolds with caustic soda solution on the A/D side and water on the E/C side. Two other feed through connections placed on the flanges are for the evacuation of the containers and the operation pressure measurement. Manifolds are integrated to the flanges for the inlet and outlet of the tube bundles heating and cooling fluid and further feed through are for the temperature sensors measuring the heating and cooling fluid temperature inside of the tube bundle tubes as well as outside of these tubes (outside tube wall temperatures).

For process and handling reasons as well as for fluid separation, both A/D and the E/C units are placed in different containers (Fig. 2). The vapour feed through connects both units, enabling the required exchanges of vapour in both directions (evaporator to absorber or desorber to condenser). On one hand the vapour pressure loss through the feed through should be as low as possible (a value between 50 and 120 Pa is expected depending on the pressure level inside of the reaction zone) and on the other hand the feed through should avoid the transfer of liquid splashes from one container to the other. Additionally, the vapour feed through should only act as mass transfer unit and therefore form a thermal barrier. A nickel plated and bended metal sheet is implemented for this task and will predominantly form a radiation shield (radiative disconnection due to the high reflectivity of the Nickel in the infrared).

In order to decrease the parasitical electrical energy consumption and to simplify the control, the A/D unit design was completed to work without fluid recirculation outside of the tubes and the E/C unit with a minimal fluid recirculation. According to the simulations, this recirculation should be able to maintain a low temperature difference (about 2 K) at the outlet of the E/C unit. Due to this water recirculation outside of the E/C tube bundle, a level sensor equipped vessel able to collect the recirculated water is required. This vessel, also named level measurement cell in Fig. 2 should avoid vainly pumping water from/to the storage tanks at each start of the reactor as well as prevent a dry running of the pump.

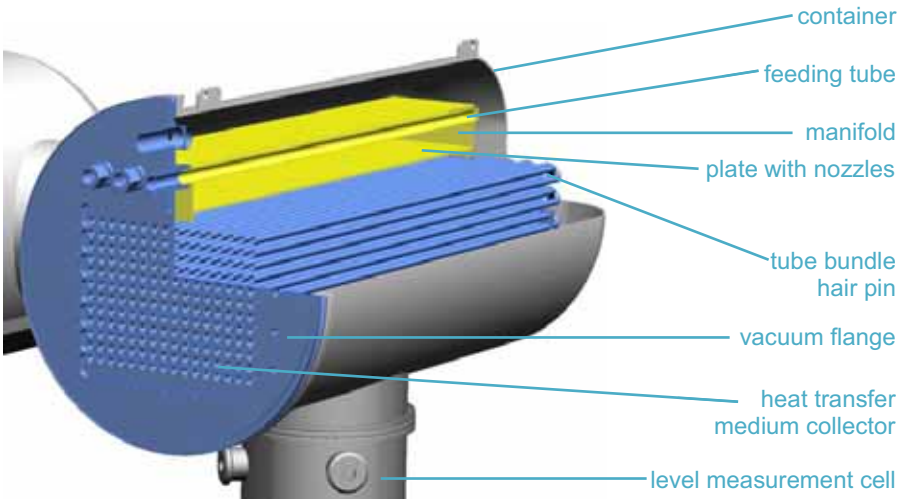

Fig. 3: CAD cross-sectional view of the E/C unit (manifold and tube bundle).

The tube bundle design is completed using tubes of 10 mm diameter. One of the criteria was that the tube bundles and manifolds (shown on the cross-sectional view from Fig. 4) should fit into a 400 mm diameter

standard vacuum tube used as container. A numerical model was developed at SPF lab and used to quantify the performances of the tube bundles (Daguenet-Frick et al. 2013).

Once the tube bundle geometry established, the next challenge was to design manifolds for a homogeneous liquid distribution taking advantage of the experimental results obtained with the preliminary test rig. Particularly tricky was the nozzles manufacturing in 1.4404 stainless steel alloy. Above several other possible designs, a version with nozzles directly machined in a stainless steel nozzles plate was retained. With this version a high flexibility on the nozzle geometry is reached, enabling a good liquid distribution. A drawback of the chosen design is that it is expensive.

Special attention was carried to the fluid distribution on the absorber/desorber tube bundle unit as this heat and mass exchanger is used without fluid recirculation. Like in the preliminary experimentation test rig, the caustic soda mixture enters the top of the manifold from both sides of a perforated feed tube. The expected pressure losses through the perforation holes are 3 to 5 time higher than those due to the fluid flow along inside the tube, ensuring an equalised fluid distribution between both ends of the manifold. A fluid film formation is aimed on the bottom plate of the manifold (the plate with the nozzles): the resulted height was between 0.5 to 0.9 mm according to the simulations and 5 to 17 mm according to estimations based on extrapolation of experimental results. Nevertheless the high discrepancy of these two results is, in all cases the formation of a liquid film on the nozzles plate will be achieved, ensuring a homogeneous fluid distribution on the manifold nozzles plate on each side of the feed tube.

For the other unit, the evaporator/condenser sorbate recirculation operation mode leads to high mass flow rates in the manifold. To limit the flow velocity and thereof the pressure loss inside the sorbate feeding tubes, a high number of tubes had to be implemented in the manifold and, due to the limited volume inside of the container envelope tube, the fluid feed could only be realised from one side of the manifold as shown on the global overview of the manifold assembly given by Fig. 4 (feed tubes - in blue, on the left - and manifold plate with the nozzles - at the bottom, placed over the tube bundle -). To ensure a homogenous distribution of the fluid all along the tube bundle, the ratio between the pressure drop through the holes of the perforated feed tubes and those due to the fluid circulation inside the tube increased to a value between 8 and 10, depending on the flow rate. According to the simulation results, a good lateral distribution of the water should also be reached by the existence of a water level height of more than 6 mm on the nozzles plate.

Fig. 4: View of the installed and measurement sensors equipped reaction zone (A/D unit left, E/C unit right). The vacuum valve - black handle - and the flexible stainless steel vacuum hose - middle right - are used for the ongoing leak test.

The described reaction zone was manufactured, assembled, equipped with sensors and connected to the rest of the facility (as shown on Fig. 4). Some preliminary tests -like Helium (He) leakage tests - preliminary to the commissioning of the seasonal heat storage are described in the next part of this paper.

3. First assessments

This part focuses on the first assessment of the A/D and E/C units in order to check their assigned functioning.

3.1. Leakage detection:

In the following a short presentation of the He-leakage test method is given and the results of our tests are shown.

The power and efficiency of closed sorption systems for thermal energy storage are -beside of others- depending of the tightness of the vacuum components contained in the whole system assembly. During operation of the sorption storage in the relevant chambers non-condensable gases like air will disturb heat and mass transfer. In a leaking vacuum chamber of volume V, the pressure p will increase continuously in time t and a leakage rate Q (in mbar*l/s, see eq. 1) can be determined (Lafferty 1998).

$$Q = \frac{V \cdot \Delta p}{\Delta t} = \frac{V \cdot \left(p(t_2) - p(t_1) \right)}{t_2 - t_1} \quad \text{(eq. 1)}$$

The leaking air (the non-condensable gas at the operating temperature T and pressure P) will hinder the heat and mass transfer in the reaction zone – and hence reduce the power Φ and efficiency of the storage unit.

There are different methods to do leakage tests on vacuum chambers (Zapfe 2007). The pressure increase method (measurement of the pressure evolution over a given duration) is the simplest one, but it does not allow the identification the exact position of the leakage, which can be a malfunction of a gasket, a pore containing welding seam, or an internal (artificial) leakage.

For an exact localization of the leakages a mass spectrometer is necessary and its sensitivity sets to the He^+ ion line with atomic mass unit 4 (*amu* = 4). In our tests we use a Pfeiffer Vacuum Mass Spectrometer QMG 220. The mass spectrometer is adapted to the vacuum chamber (see Fig. 5) and separately pumped by a turbo and a mechanical pump to reach operation pressure lower than $p=1*10^{-4}$ mbar as at higher pressures operation the spectrometer is damaged. If required (if too significant leakage), a sintered micro-porous filter is inserted between the tested container and the mass spectrometer to ensure the low enough operation pressure. During the leakage test, while the outside wall of the tested container is locally sprayed with Helium, the ion current I is measured in function of time t. The quadrupole mass spectrometer measures the He^+ line inside of the tested container. Each peak in the measurement curve means an increase of the He^+ intensity betraying the location of a leakage.

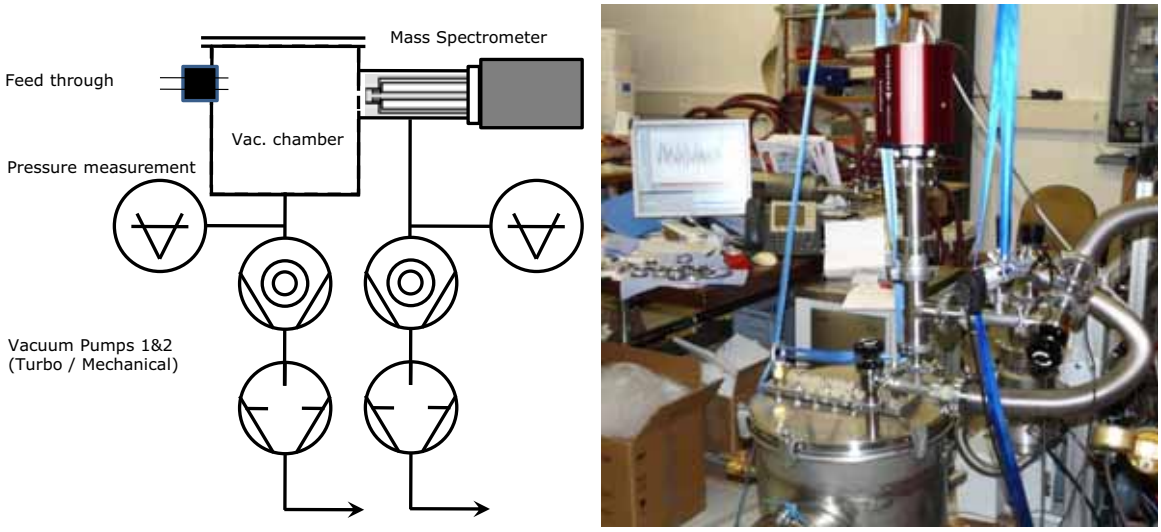

Fig. 5: Principle schematic of a leakage test with mass spectrometer (left) and setup of the He leakage tests with an Pfeiffer QMG 220 (right).

In this context, Helium leakage tests were carried out for each of the different components constituting the reaction zone. Most of the detected leakages were located at temperature sensor feed through (flat gaskets) but some were also located at the junction of standard vacuum elements (damaged die spit) and one on a

welding seam.

After repairing of the leakages, rest gas spectra were taken with the same spectrometer to identify the "contaminating" gases in the vacuum chambers.

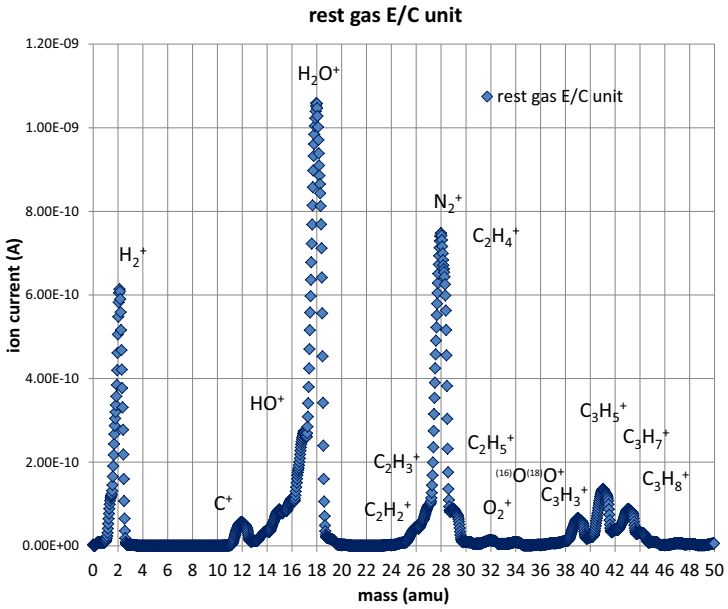

Fig. 6: Rest gas spectrum of the E/C unit.

According to Fig. 6, apart from hydrogen (typical to vacuum application) and nitrogen (air main constituent), the rest gas consists of water (H_2O vapour) and of hydro-carbons (C_nH_{2n+2} vapour) stemming from the vacuum chamber surfaces.

3.2. Wetting measurements

For a check of the efficiency of the A/D unit manifold, an optical setup was realized (see Fig. 7). In this experiment, the working fluid pumped by a dosing pump flows through a nozzle manifold from top to down over the tested tube bundle (see Fig. 8). The flow pattern is measured by a CCD camera taking and averaging pictures to a mean representation.

An optical method was developed to quantify the wetting of the heat and mass exchanger tube arrangement. While the fluid flows downward over the tube bundle pictures of the heat and mass exchanger tubes are taken with the CCD camera. The tubes are illuminated from the front (spotlight) and from the back side (diffuse backlight) as showed on Fig. 7. On the obtained pictures, the dark areas between the tubes show the presence of fluid droplets. In order to ensure a high repeatability of the calculated tube bundle surface wetting fraction, statistics is done on sets of 1000 pictures taken at a frequency of 2 Hz and with an exposition aperture opening time of 10 µs per single photo.

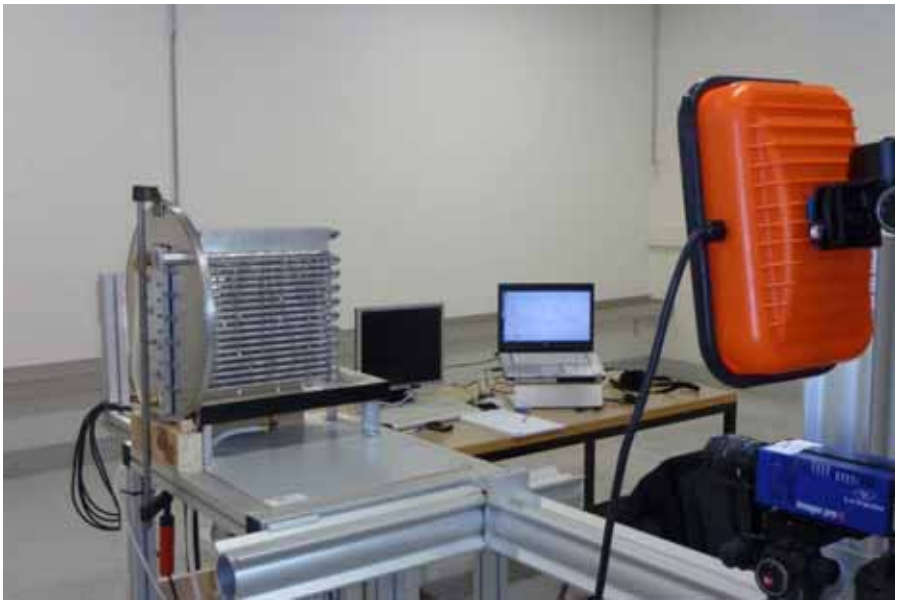

Fig. 7: View of the A/D heat and mass heat exchanger during the fluid distribution test.

Profiles giving the recorded light intensity in the gap between two tubes are extracted from the post-processed pictures in order to find the fluid distribution along the tube bundle. A light intensity threshold is set and the presence of fluid determined by a Boolean operation, leading to the determination of a wet surface fraction indicator (ratio of the length where fluid is detected by the total tube length). Thanks to the profiles set up at the top of the tube bundle (directly under the manifold), the validation of a good functioning of the absorber/desorber manifold was achieved: on two measurements campaigns (impinging mass flow rate range between 1 and 30 l/h), the average relative difference on the wet surface fraction indicator between left and right part of the tube bundle is about 5%. Fig. 8 shows the proper working of the manifold with water as working fluid: the droplets are properly falling under the nozzles and hit the upper tubes of the tube bundle on their total length. As shown by the preliminary work on a downscaled experiment, the replacement of water by caustic soda should not be any problem (Daguenet-Frick et al. 2013).

Fig. 8: Side view of the falling film on the A/D tube bundle heat and mass exchanger (left) and instrumented – temperature sensors - A/D tube bundle (right); impinging mass flow rate: 30 l/h of water.

Three different measurement campaigns were performed on the absorber/desorber tube bundle in order to determine the evolution of the wet surface fractions indicator. In these campaigns the impinging mass flow rates was extended to the foreseen working range of this heat and mass exchanger (see Fig. 9). One further aim was to check the influence of the temperature sensors mounted outside of the tubes (film temperature

measurement, see Fig. 8, right) on the fluid flow. Averaged values from two measurement campaigns without sensors on the tube bundle were used to determine the three curves (18^{th}_avg, 10^{th}_avg and 6^{th}_avg) presented in Fig. 9. At least at the top of the tube bundle, logarithmic trend-lines (curves in black on Fig. 9) fit well with the measurement data. For a considered mass flow rate, from the top to the middle of the tube bundle, a decrease of the wet surface fraction can be observed. It seems that this phenomenon is reversed at the bottom of the tube bundle. In this part of the tube bundle, a minor increase of the wet surface fraction is observed while the mass flow rate increased to values higher than 15 l/h.

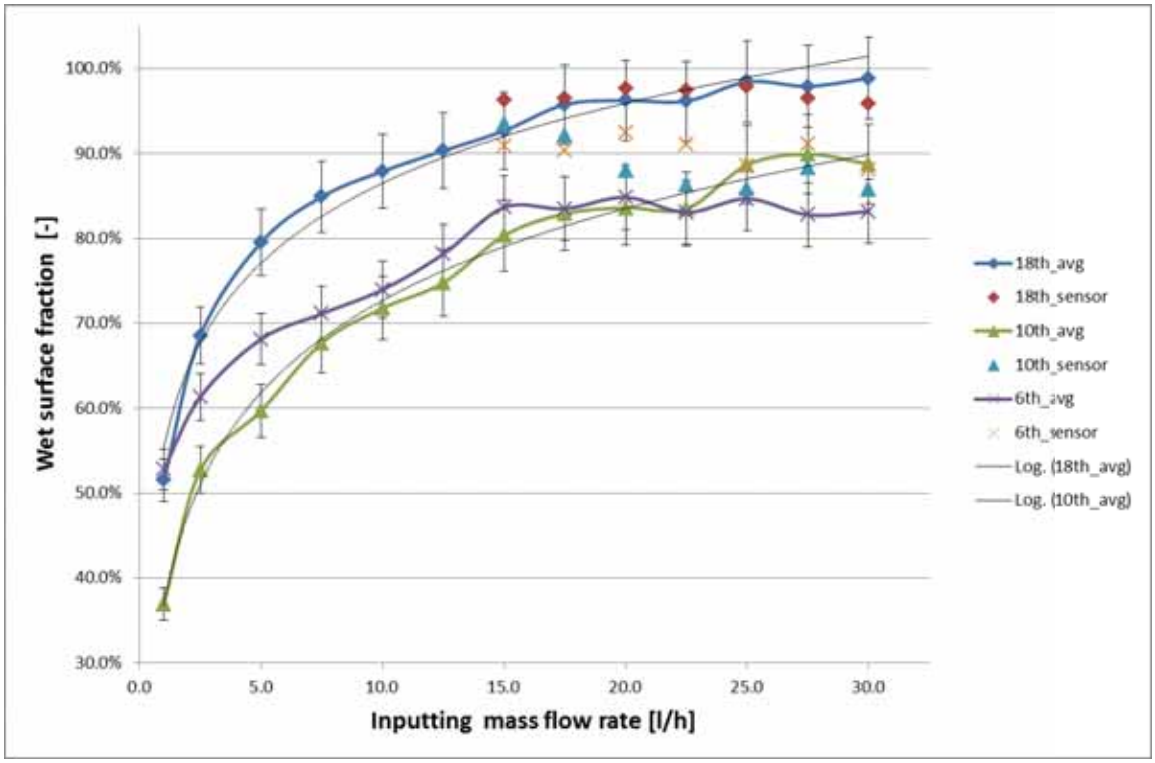

Fig. 9: Development of the tube bundle wet surface fraction in function of the mass flow rate at different positions (18^{th} row: top of the tube bundle; 6^{th} row: bottom of the tube bundle).

In Fig. 10, focus is put on the influence of the position along the tube bundle on the wet surface fraction (measurements were achieved with mass impinging flow rates between 20 and 30 l/h, mass flow rate range in which the dependence of the wet surface fraction on the impinging mass flow rate is low). The graph in Fig. 10 shows, as supposed previously, that the highest value of the wet surface fraction is reached at the top of the tube bundle, directly under the manifold. By trickling down the first 12 tubes, some of the droplets coalesce, leading to a decrease of the wet surface fraction. After this happen, the trend is apparently reversed, leading to a little increase of the wet surface fraction. This phenomenon, confirmed by inspection of the post processed pictures was not noticed during the preliminary experiments as the tube bundle height was to low (6 tubes rows) - to notice such an evolution.

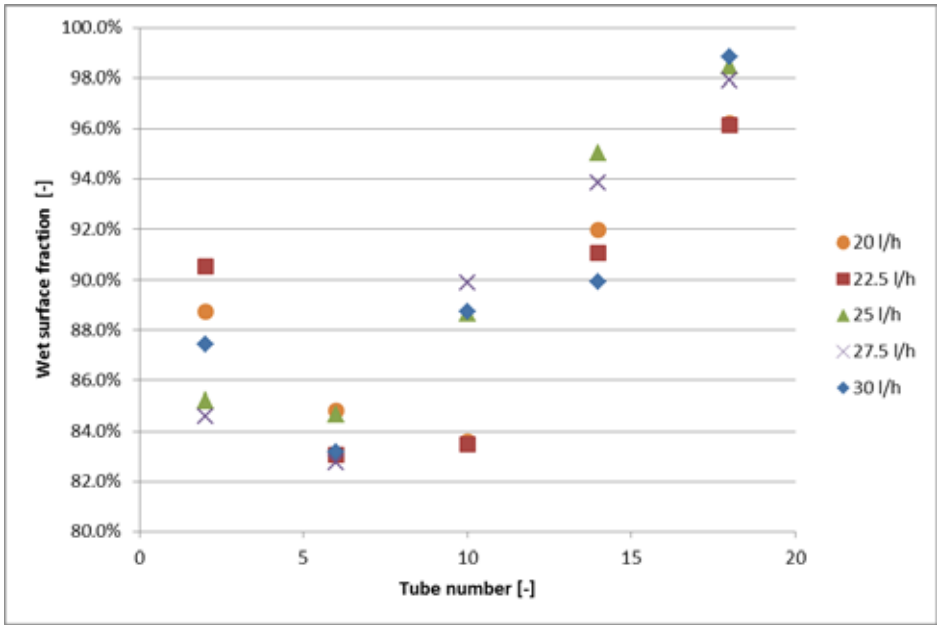

Fig. 10: Development of the tube bundle wet surface fraction in function of the position along the tube bundle for different mass flow rates.

In Fig. 9, the three lasts series of points (*18th_sensor*, *10th_sensor* and *6th_sensor*) are measurement obtained after the installation of the temperature sensors and in the upper mass flow rate domain (working range of the absorber/desorber). At the top of the tube bundle, the influence of these sensors on the flow pattern seems to be negligible (measures within the range of the uncertainty bars) whereas at the bottom a noticeable increase (about 8 %) can be seen. To summarize, the installation of temperature sensors should not disturb the flow pattern and thus the performances of the heat and mass exchangers.

4. Conclusion

The thermochemical seasonal storage demonstrator reaction zone design is based on two tube bundle heat and mass exchangers placed in two separate vacuum containers connected by a vapour feed through tube. In fact, the seasonal sequential running of the heat storage allows the combination of the absorber and of the desorber in one unit as well as of the evaporator and of the condenser in a second one. The design is carried out in order to have easy access to the tube bundles and their accessories (maintenance) and to have a good sight to the process (fluid distribution & control). For a low air leakage rate the number of sealing gaskets is kept as low as possible (vacuum tight facility). Special attention was paid to the manifold concept and to its design in order to ensure an optimal working of the heat and mass exchanger (fluid equally distributed all along the tubes).

Before integrating the reaction zone in the demonstrator facility, a preliminary assessment was carried out: First, Helium leakage tests enabled us to find and repair all the major leakages. The second step was to validate the manifolds functioning and to be sure that the temperature sensors clamped outside of the tubes constituting the tube bundle do not severely disturb the fluid flow, which was proved in an optical study of the flow profile on the Absorber/Desorber unit within a wide mass flow rate range.

The reaction zone described in the present study was developed in the frame of the EU project COMTES and will be integrated in a demonstrator facility able to supply heat and domestic hot water to a typical low consumption single family house.

Acknowledgment - Financial support by the European Union in the frame of FP 7 under the grant number 295568 and the University of Applied Sciences Rapperswil and the Swiss Federal Laboratories for Materials Science and Technology is gratefully acknowledged.

5. References

Daguenet-Frick, X., Gantenbein, G., Frank, E., Weber, R., Fumey, B. and Williamson, T., 2013. "Reaction Zone Development for an Aqueous Sodium Hydroxide Seasonal Thermal Energy Storage." In ISES Solar World Congress, Cancun, Mexico.

Duffie, J.A. and Beckman, W.A,. 2013. Solar Engineering of Thermal Processes. John Wiley & Sons.

Fumey, B., Weber, R., Gantenbein, P., Daguenet-Frick, X., Williamson, T. and Dorer, V., 2014. "Development of a Closed Sorption Heat Storage Prototype." Energy Procedia, 8th International Renewable Energy Storage Conference and Exhibition (IRES 2013), 46: 134–41. doi:10.1016/j.egypro.2014.01.166.

Lafferty, J.M., 1998. Foundations of Vacuum Science and Technology. Wiley.

Weber, R., and Dorer, V., 2008. "Long-Term Heat Storage with NaOH." Vacuum 82 (7): 708–16. doi:10.1016/j.vacuum.2007.10.018.

Zapfe, K., 2007. Leak Detection. Technical Note. Hamburg, Germany: Deutsches Elektronen-Synchrotron DESY. http://www.desy.de/~ahluwali/technicalnotes/2007_03.pdf.